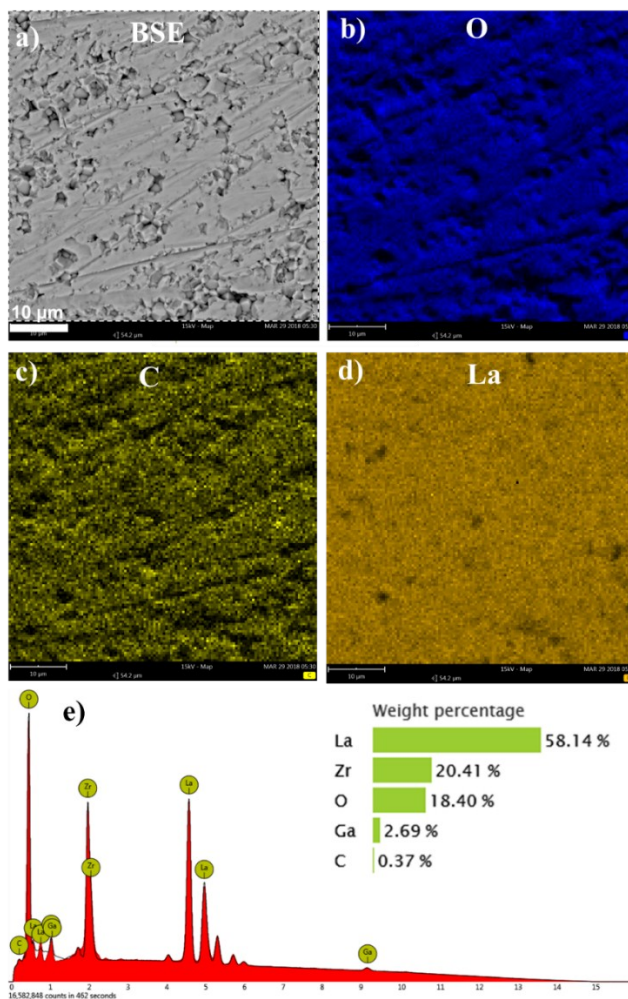


Electronic Supplementary Information for

The Role of Solid Electrolyte Interphase Layer in Preventing Li Dendrite Growth in Solid-State Batteries

Bingbin Wu,^a ‡ Shanyu Wang,^b ‡ Joshua Lochala,^a David Desrochers,^a Bo Liu,^c Wenqing Zhang,^d Jihui Yang,^{b*} and Jie Xiao^{ae*}



a. Department of Chemistry and Biochemistry, University of Arkansas, Fayetteville, AR 72701, USA. Email: jixiao@uark.edu
b. Materials Science and Engineering Department, University of Washington, Seattle, WA 98195, USA. E-mail: jihuiy@uw.edu
c. Materials Genome Institute, Shanghai University, Shanghai 200444, China
d. Department of Physics, Southern University of Science and Technology, 1088 Xueyuan Rd., Shenzhen, Guangdong, 518055, China
e. Pacific Northwest National Laboratory, Richland, WA 99252, USA
‡ These authors contributed equally to this work.

Fig. S1 Phase and composition of fresh LLZO. a) Back scattered image; b)-d) elemental mapping of O, C, and La; e) EDS spectrum and element weight percentage.

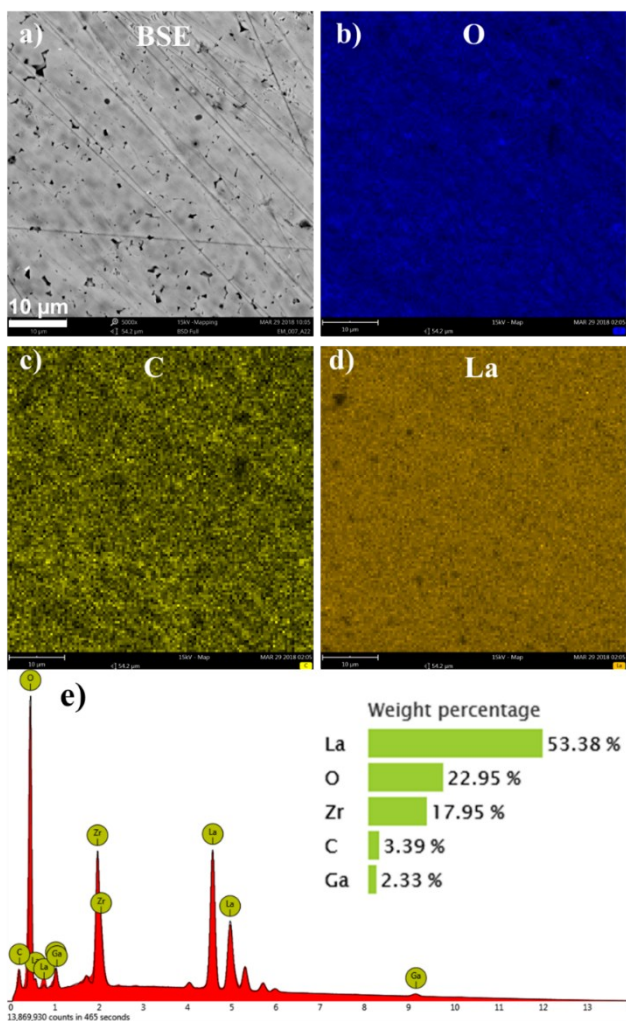


Fig. S2 Phase and composition of LLZO after exposed in lab environment (20 °C, 40% relative humidity) for 3 days. a) Back scattered image; b)-d) elemental mapping of O, C, and La; e) EDS spectrum and elemental weight percentage.

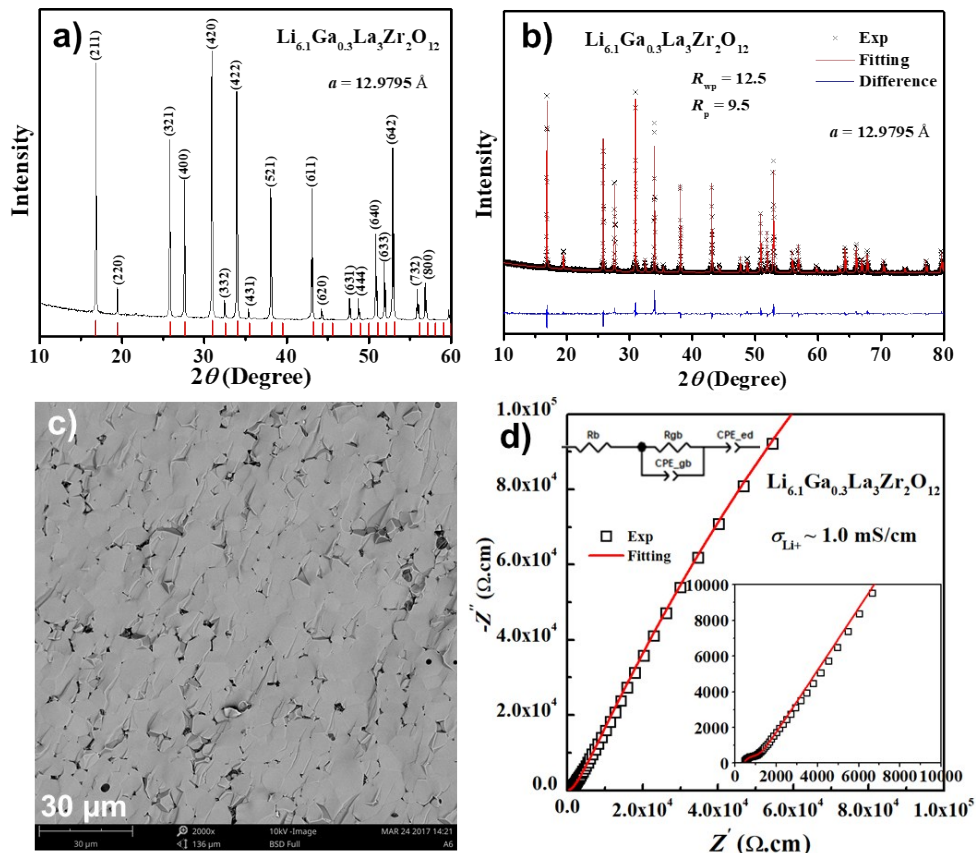


Fig. S3 a) XRD pattern and b) refinement; c) SEM image of fractural surface; d) Electrochemical Impedance Spectroscopy data (Nyquist Plot) of $\text{Li}_{6.1}\text{Ga}_{0.3}\text{La}_3\text{Zr}_2\text{O}_{12}$. The inset in d) shows the equivalent circuit used for Nyquist plot fitting, which consists of a serial combination of bulk resistance R_b , grain boundary resistance R_{gb} (paralleled with a constant phase element CPE_{gb}), and constant phase element CPE_{ed} representing the ion-blocking effect of Ag electrodes. The ionic conductivity $\text{Li}_{6.1}\text{Ga}_{0.3}\text{La}_3\text{Zr}_2\text{O}_{12}$ is estimated to be 1.0 mS cm^{-1} according to the $\sigma = L / (R_b \cdot A)$, where σ is the ionic conductivity of the LLZO, L is the thickness of the LLZO pellet and A is its area.

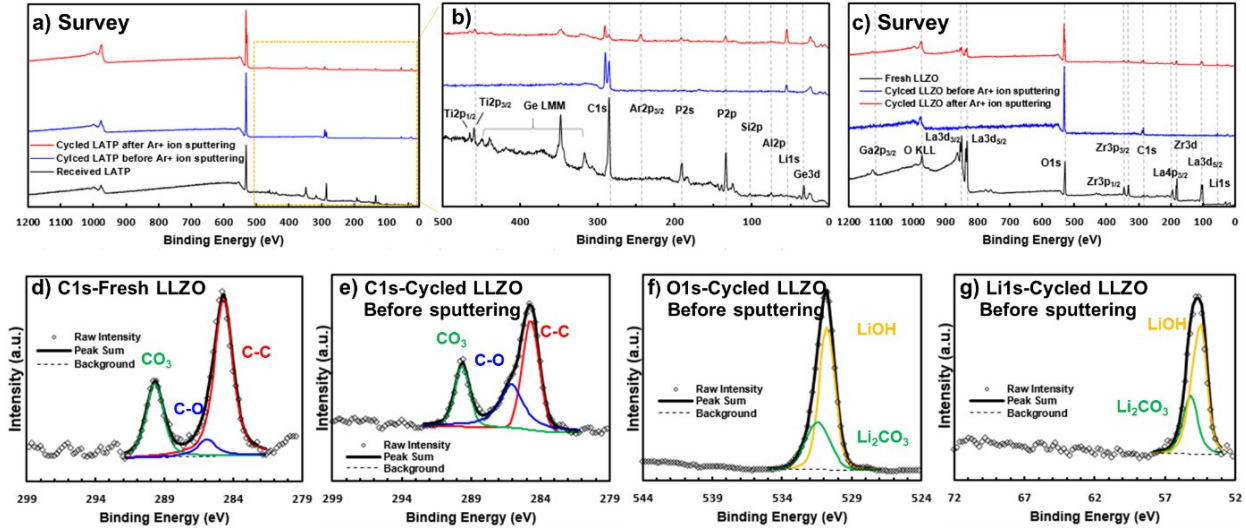


Fig. S4 XPS full survey of both fresh and cycled a) LTP and c) LLZO with or without an Ar⁺ ion sputtering. b): enlarged image of (a) with the binding energy ranges from 0 to 500 eV; (d): C 1s spectra of fresh LLZO; e-g): C 1s, O 1s, and Li 1s spectra of the cycled LLZO before Ar⁺ ion sputtering.

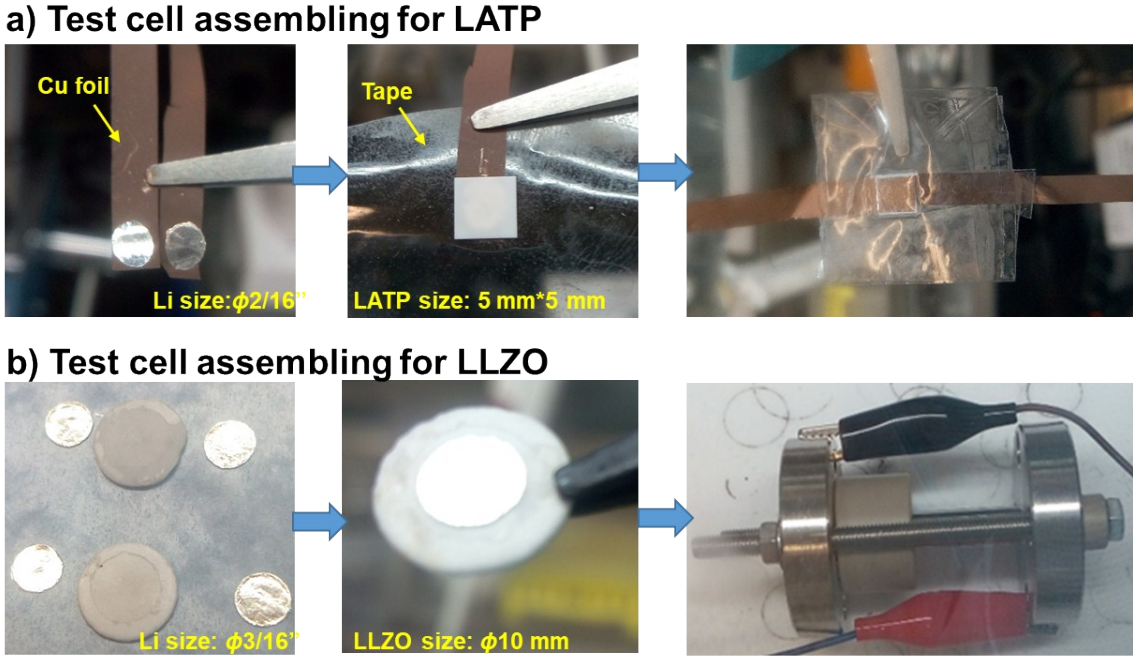


Fig. S5 Structures and assembling processes of a) Li/LTP/Li and b) Li/LLZO/Li symmetric cells.

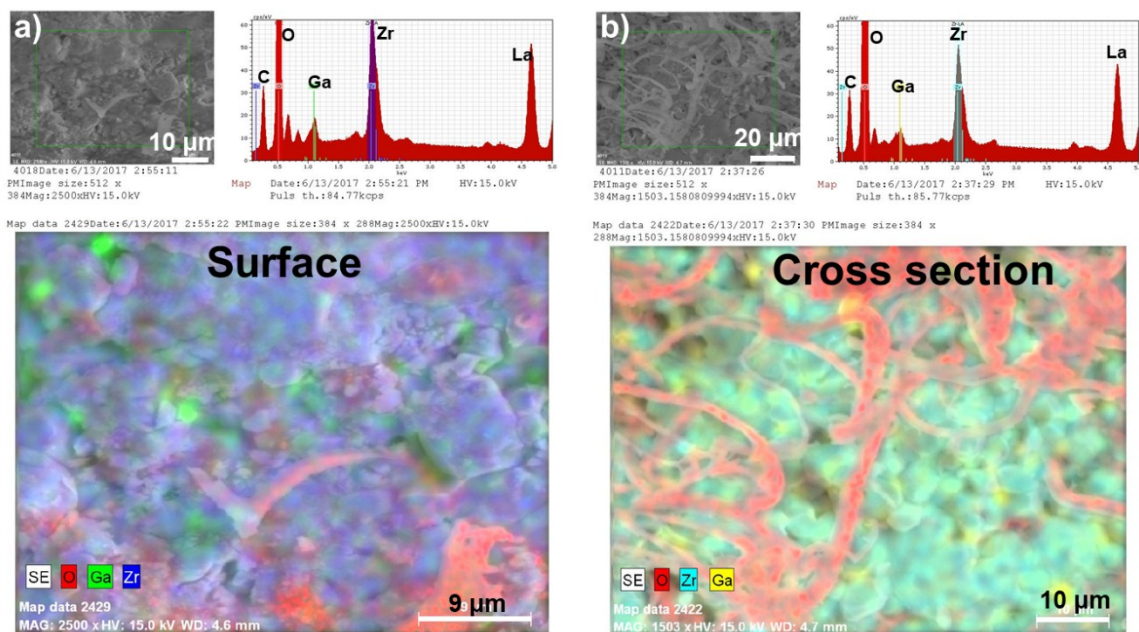


Fig. S6 EDS mapping of cycled LLZO after exposed in the air for 3 days. a) Surface; b) Cross section. O, Ga, and Zr were detected and analyzed.

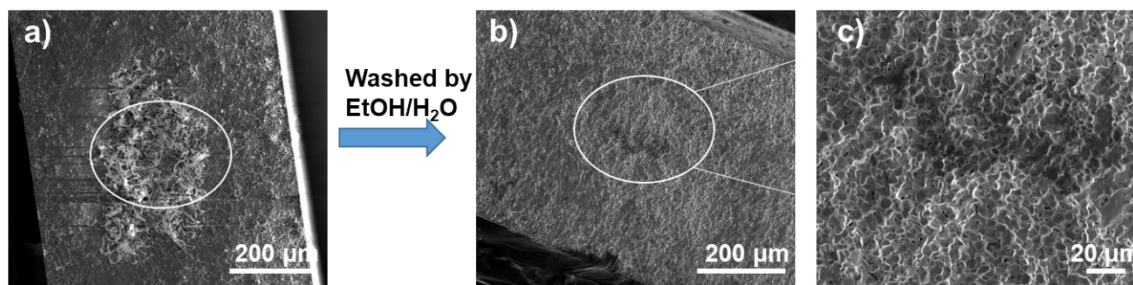
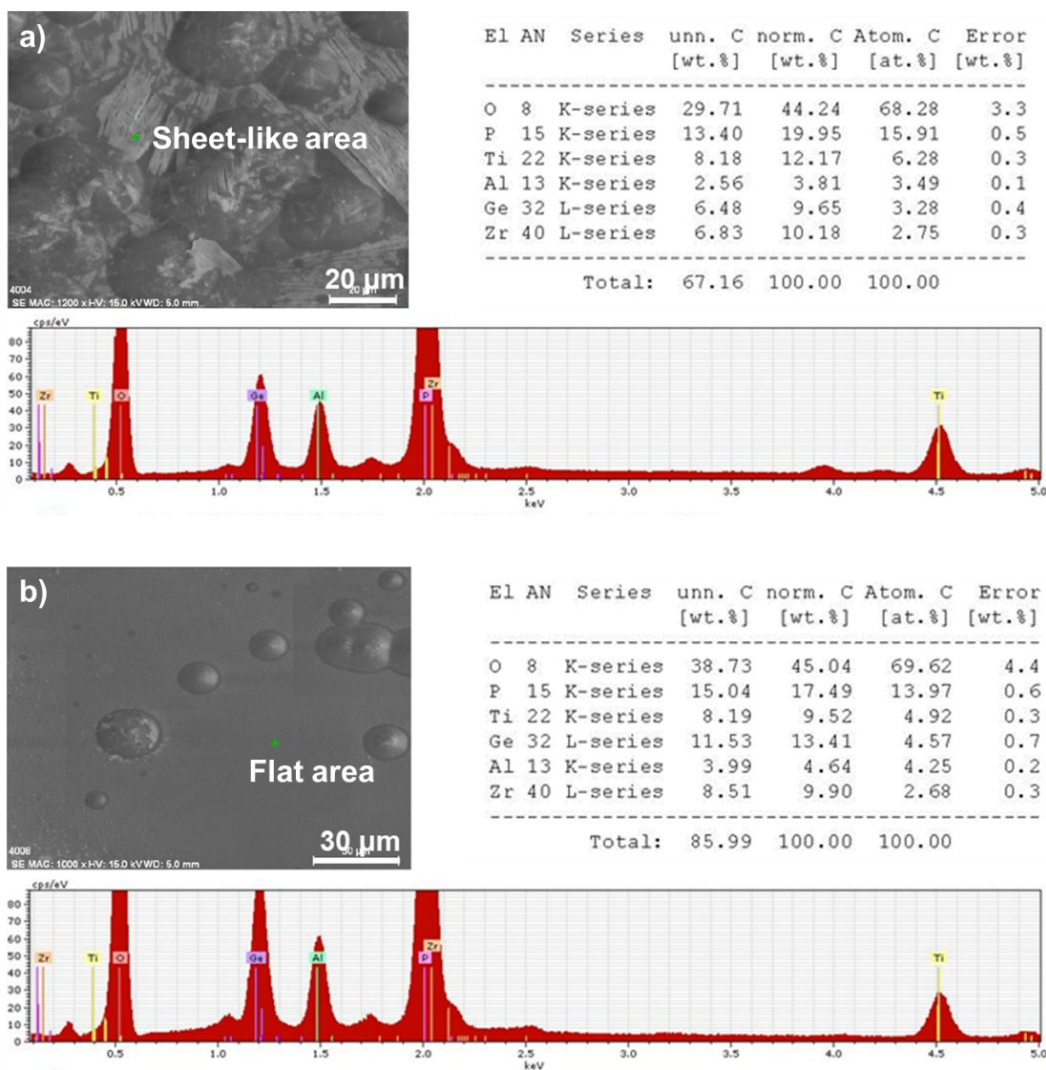


Fig. S7 SEM images of the cycled LLZO after exposed in the air for 3 days (a) (same image in Fig. 3c) and then washed by EtOH/H₂O (b) and its enlarged image (c). The fibers in (a) were completely removed after washed by EtOH/H₂O.



c)

Elements	Atomic percentage [at.%]	
	Sheet-like area in Fig. S8a	Flat area in Fig. S8b
O	68.28	69.62
P	15.91	13.97
Ti	6.28	4.92
Al	3.49	4.25
Ge	3.28	4.57

Fig. S8 EDS analysis of the cycled LTP surface after exposed in the air for 3 days. a) Sheet-like area; b) Flat area. O, P, Ti, Al, and Ge were detected and analyzed. c) Comparison of atomic percentages of the sheet-like area in (a) and flat area in (b).

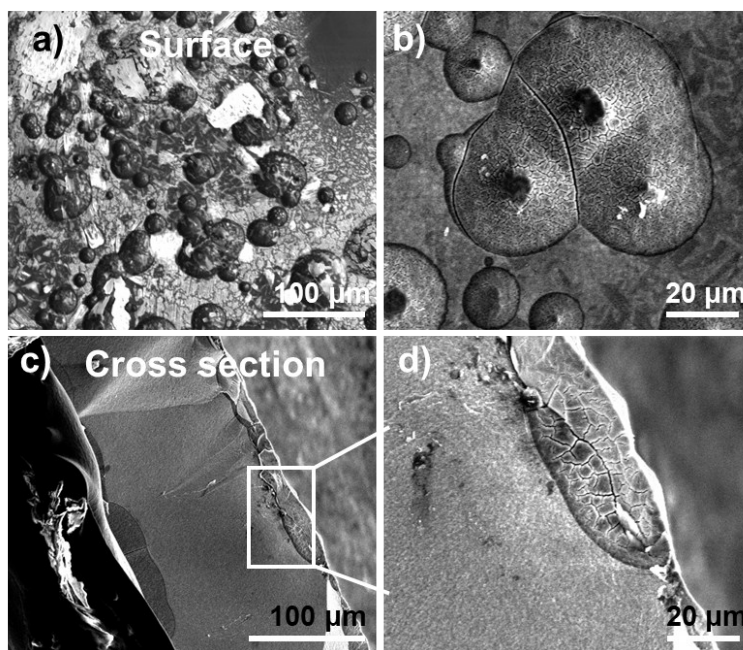


Fig. S9 SEM morphologies of a, b) surface and c, d) cross section of the cycled LATP in a lithium symmetric cell washed by EtOH/H₂O.

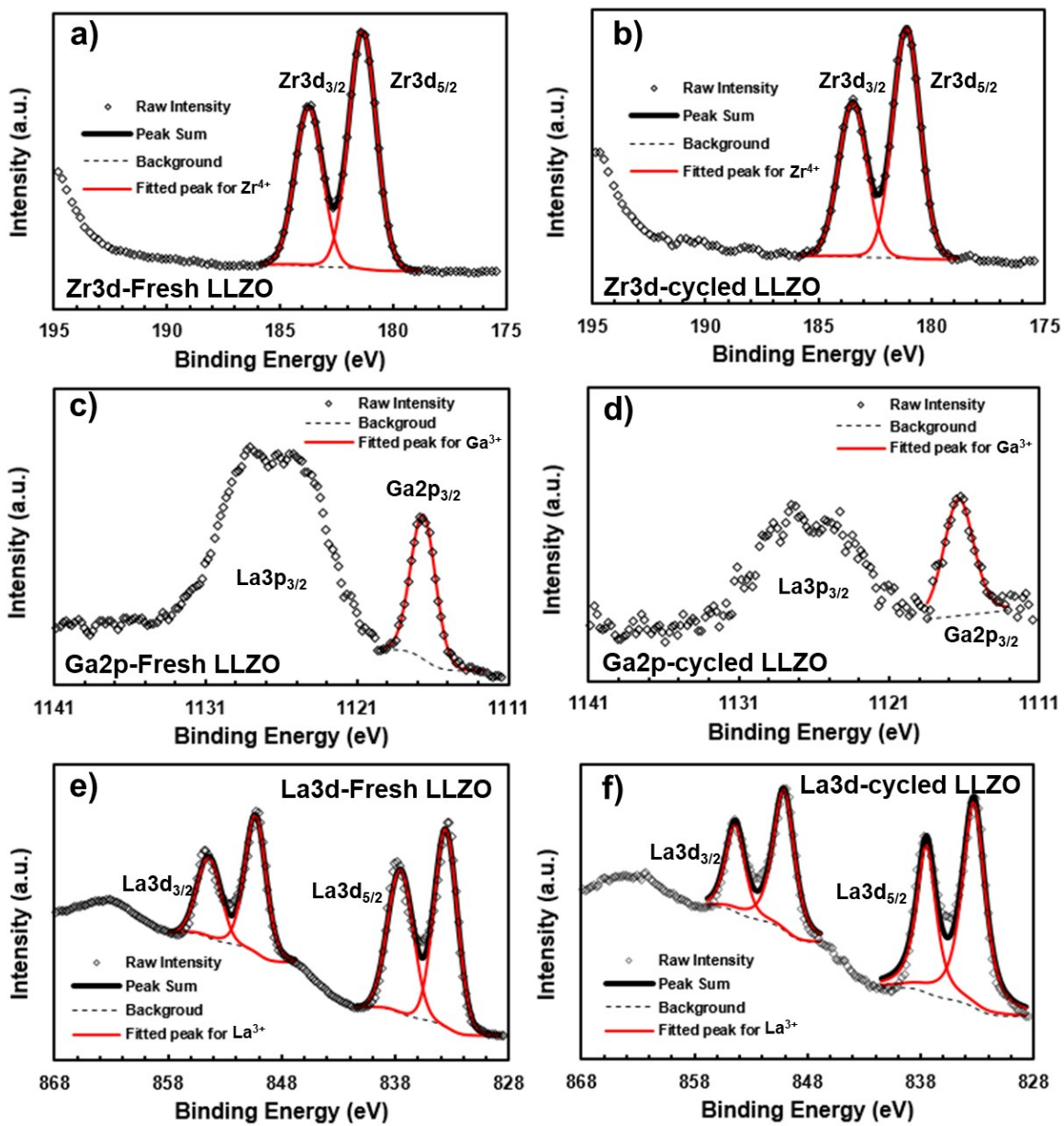


Fig. S10 XPS results of a, b) Zr 3d, c, d) Ga 2p, and e, f) La 3d of LLZO before and after cycled in a Li/LLZO/Li symmetric cell.

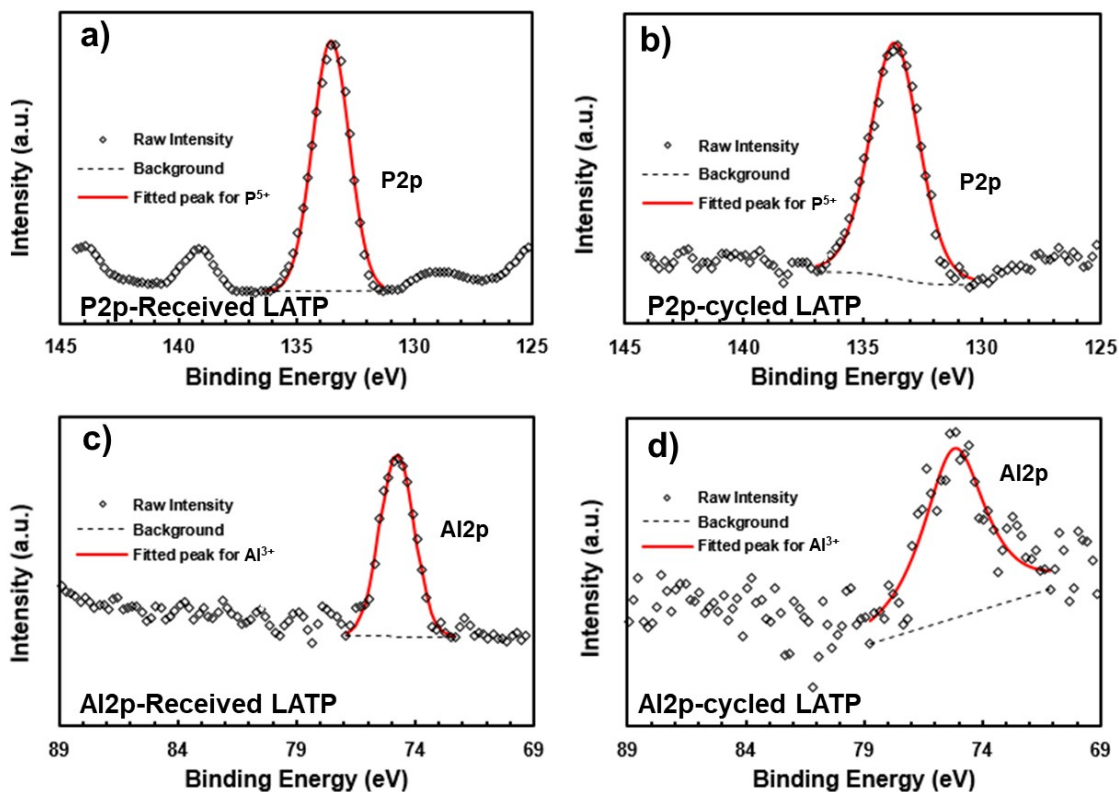


Fig. S11 XPS results of a, b) P 2p and c, d) Al 2p of LAMP before and after cycled in a Li/LAMP/Li symmetric cell.

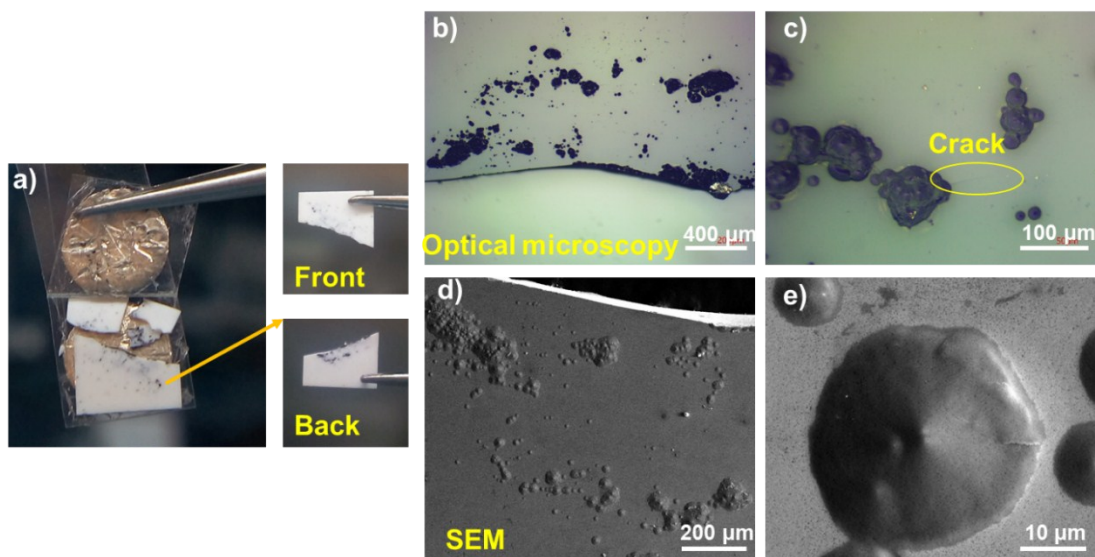


Fig. S12 a) Digital images of LAMP directly contacted with Li metal for 3 days, upright is the front image of the broken LAMP piece while the downright is the back. b, c): Optical images of the surface of LAMP after contacted with Li metal; d, e): SEM images of the surface of LAMP after contacted with Li metal.

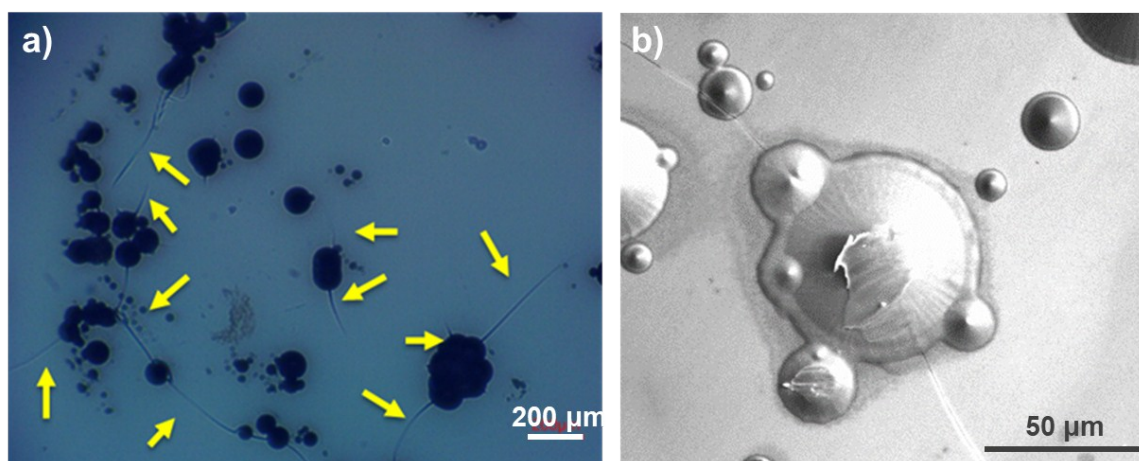


Fig. S13 a) Optical and b) SEM images of cracks on the surface of LATP after cycled in a lithium symmetric cell.

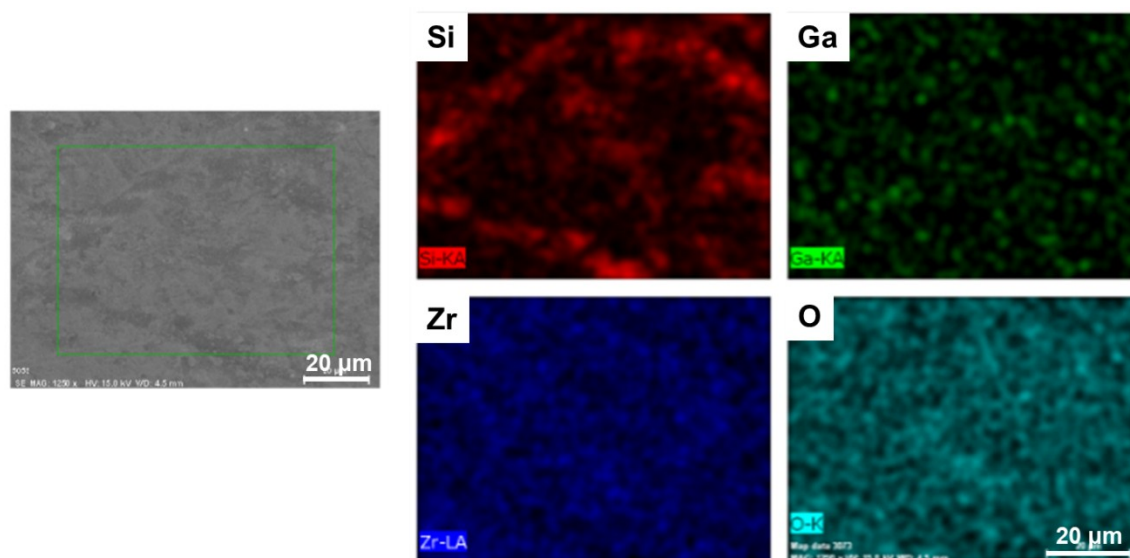


Fig. S14 EDS mapping of nano-Si polished LLZO. EDS mapping of Si, Ga, Zr and O were shown.

Table S1. Summary of XPS fitting results for LATP and LLZO before and after cycled in lithium symmetric cells.

SSEs	State	Element	Spectral Line	Binding Energy (eV)	FWHM (eV)	Area Ratio (%) ^{a)}
LATP	Fresh	Ti	Ti2p _{1/2} (Ti ⁴⁺)	465.2	1.98	33.3
			Ti2p _{3/2} (Ti ⁴⁺)	459.4	1.33	66.7
		Ge	Ge3d (Ge ⁴⁺)	32.7	1.53	100
		Al	Al2p (Al ³⁺)	74.8	1.71	100
		P	P2p (P ⁵⁺)	133.5	1.83	100
	Cycled	Ti	Ti2p _{1/2} (Ti ⁴⁺)	464.3	2.15	21.1
			Ti2p _{3/2} (Ti ⁴⁺)	458.6	2.12	42.1
			Ti2p _{1/2} (Ti ³⁺)	462.6	1.91	12.3
		Ge	Ti2p _{3/2} (Ti ³⁺)	457.2	1.77	24.5
			Ge3d (Ge ⁴⁺)	32.9	1.55	91.2
			Ge3d (Ge ²⁺)	31.1	1.13	8.8
		Al	Al2p (Al ³⁺)	75.2	3.14	100
		P	P2p (P ⁵⁺)	133.6	2.42	100
		LLZO	Fresh	Zr	Zr3d _{3/2} (Zr ⁴⁺)	183.7
Zr3d _{5/2} (Zr ⁴⁺)	181.3				1.44	60.7
Ga	Ga2p _{3/2} (Ga ³⁺)			1116.6	1.93	100
La ^{b)}	La3d _{5/2} (La ³⁺)			833.5	2.42	56.5
				837.5	2.65	43.5
Cycled	Zr		Zr3d _{3/2} (Zr ⁴⁺)	183.5	1.48	40.6
			Zr3d _{5/2} (Zr ⁴⁺)	181.1	1.43	59.4
	Ga		Ga2p _{3/2} (Ga ³⁺)	1116.4	2.34	100
	La		La3d _{5/2} (La ³⁺)	833.3	2.39	61.5
				837.5	2.05	38.5

a) Area ratio was normalized by the total area of each spectral line related to each element.

b) Doublet peak of La3d_{5/2} by spin-orbit splitting with 4.0 eV of ΔE .

Table S2. Phase equilibria and Gibbs free energies of Li and $\text{Li}_{6.25}\text{Ga}_{0.25}\text{La}_3\text{Zr}_2\text{O}_{12}$

Phase Equilibria ^{a)}	ΔG (eV)
$\text{Li}_5\text{GaO}_2, \text{ZrO}_2, \text{La}_2\text{O}_3, \text{Li}_2\text{O}$	2.69
$\text{Li}_2\text{Zr}_2\text{O}_7, \text{La}_4\text{Ga}_2\text{O}_9, \text{La}_5\text{GaO}_2, \text{La}_2\text{O}_3, \text{Li}_2\text{O}$	2.38
$\text{Li}_2\text{Zr}_2\text{O}_7, \text{La}_4\text{Ga}_2\text{O}_9, \text{LaZr}_2\text{O}_4, \text{La}_2\text{O}_3, \text{Li}_2\text{O}$	2.82
$\text{Li}_2\text{Zr}_2\text{O}_7, \text{La}_4\text{Ga}_2\text{O}_9, \text{LiZrO}_2, \text{La}_2\text{O}_3, \text{Li}_2\text{O}$	3.22
$\text{Li}_2\text{Zr}_2\text{O}_7, \text{La}_4\text{Ga}_2\text{O}_9, \text{Li}_3\text{ZrO}_3, \text{La}_2\text{O}_3, \text{Li}_2\text{O}$	2.76
$\text{La}_2\text{Zr}_2\text{O}_7, \text{La}_3\text{Ga}_5\text{O}_{12}, \text{Li}_5\text{GaO}_2, \text{La}_2\text{O}_3, \text{Li}_2\text{O}$	7.90
$\text{La}_2\text{Zr}_2\text{O}_7, \text{La}_3\text{Ga}_5\text{O}_{12}, \text{LiZrO}_2, \text{La}_2\text{O}_3, \text{Li}_2\text{O}$	7.74
$\text{La}_2\text{Zr}_2\text{O}_7, \text{La}_3\text{Ga}_5\text{O}_{12}, \text{Li}_3\text{ZrO}_3, \text{La}_2\text{O}_3, \text{Li}_2\text{O}$	7.28
$\text{La}_2\text{Zr}_2\text{O}_7, \text{La}_3\text{Ga}_5\text{O}_{12}, \text{LiZr}_2\text{O}_4, \text{La}_2\text{O}_3, \text{Li}_2\text{O}$	8.34

a) Li and LLZO reactions involved in related phase equilibria above:

- $4\text{Li}_{6.25}\text{Ga}_{0.25}\text{La}_3\text{Zr}_2\text{O}_{12} + 4\text{Li} \rightarrow \text{Li}_5\text{GaO}_2 + 8\text{ZrO}_2 + 6\text{La}_2\text{O}_3 + 12\text{Li}_2\text{O}$
 $\Delta G = 2.69 \text{ eV}$
- $12\text{Li}_{6.25}\text{Ga}_{0.25}\text{La}_3\text{Zr}_2\text{O}_{12} + 4\text{Li} \rightarrow 12\text{Li}_2\text{Zr}_2\text{O}_7 + \text{La}_4\text{Ga}_2\text{O}_9 + \text{La}_5\text{GaO}_2 + 4\text{La}_2\text{O}_3 + 37\text{Li}_2\text{O}$
 $\Delta G = 2.38 \text{ eV}$
- $8\text{Li}_{6.25}\text{Ga}_{0.25}\text{La}_3\text{Zr}_2\text{O}_{12} + \text{Li} \rightarrow 7\text{Li}_2\text{Zr}_2\text{O}_7 + \text{La}_4\text{Ga}_2\text{O}_9 + \text{LaZr}_2\text{O}_4 + 3\text{La}_2\text{O}_3 + 25\text{Li}_2\text{O}$
 $\Delta G = 3.35 \text{ eV}$
- $8\text{Li}_{6.25}\text{Ga}_{0.25}\text{La}_3\text{Zr}_2\text{O}_{12} + 2\text{Li} \rightarrow 7\text{Li}_2\text{Zr}_2\text{O}_7 + \text{La}_4\text{Ga}_2\text{O}_9 + 2\text{LiZrO}_2 + 3\text{La}_2\text{O}_3 + 25\text{Li}_2\text{O}$
 $\Delta G = 3.75 \text{ eV}$
- $8\text{Li}_{6.25}\text{Ga}_{0.25}\text{La}_3\text{Zr}_2\text{O}_{12} + 2\text{Li} \rightarrow 7\text{Li}_2\text{Zr}_2\text{O}_7 + \text{La}_4\text{Ga}_2\text{O}_9 + 2\text{Li}_3\text{ZrO}_3 + 3\text{La}_2\text{O}_3 + 23\text{Li}_2\text{O}$
 $\Delta G = 3.77 \text{ eV}$
- $24\text{Li}_{6.25}\text{Ga}_{0.25}\text{La}_3\text{Zr}_2\text{O}_{12} + 4\text{Li} \rightarrow 24\text{La}_2\text{Zr}_2\text{O}_7 + \text{La}_3\text{Ga}_5\text{O}_{12} + \text{Li}_5\text{GaO}_2 + 10.5\text{La}_2\text{O}_3 + 74.5\text{Li}_2\text{O}$
 $\Delta G = 7.90 \text{ eV}$
- $20\text{Li}_{6.25}\text{Ga}_{0.25}\text{La}_3\text{Zr}_2\text{O}_{12} + 2\text{Li} \rightarrow 19\text{La}_2\text{Zr}_2\text{O}_7 + \text{La}_3\text{Ga}_5\text{O}_{12} + 2\text{LiZrO}_2 + 9.5\text{La}_2\text{O}_3 + 62.5\text{Li}_2\text{O}$
 $\Delta G = 8.27 \text{ eV}$
- $20\text{Li}_{6.25}\text{Ga}_{0.25}\text{La}_3\text{Zr}_2\text{O}_{12} + 2\text{Li} \rightarrow 19\text{La}_2\text{Zr}_2\text{O}_7 + \text{La}_3\text{Ga}_5\text{O}_{12} + 2\text{Li}_3\text{ZrO}_3 + 9.5\text{La}_2\text{O}_3 + 60.5\text{Li}_2\text{O}$
 $\Delta G = 8.29 \text{ eV}$
- $20\text{Li}_{6.25}\text{Ga}_{0.25}\text{La}_3\text{Zr}_2\text{O}_{12} + \text{Li} \rightarrow 19\text{La}_2\text{Zr}_2\text{O}_7 + \text{La}_3\text{Ga}_5\text{O}_{12} + \text{LiZr}_2\text{O}_4 + 9.5\text{La}_2\text{O}_3 + 62.5\text{Li}_2\text{O}$
 $\Delta G = 8.87 \text{ eV}$

It is worth mentioning that the products Li_3ZrO_3 , LiZrO_2 , and LiZr_2O_4 in formulas 3, 4, 5, 7, 8, and 9 can be further decomposed into ZrO_2 , ZrO_3 , and Li_2ZrO_3 , etc., but this will neither change the Gibbs free energies much nor the overall conclusion.